ACADEMIA ROMÂNĂ
Revue Roumaine de Chimie
https://www.icf.ro/rrch/

Rev. Roum. Chim.,
2023, *68*(10–12), 507–513
DOI: 10.33224/rrch.2023.68.10-12.02

THREE DIMENSIONS ADVECTION-DIFFUSION EQUATION IN UNSTABLE CONDITION

Khaled S. M. ESSA and Sawsan E. M. EL SAID*

Mathematics and Theoretical Physics, Nuclear Research Center, Egyptian Atomic Energy Authority, Cairo-Egypt

Received August 7, 2022

The advection-Diffusion Equation in three dimensions was solved using the Separation variable, Substitution and Laplace transform methods, taking into account that eddy diffusivity along the horizontal, lateral coordinates and wind velocity are constant respectively, while the vertical eddy diffusivity is a function of the vertical height *z*, Monin-Obukhov length *L* friction velocity at different emission rate and operation of iodine (I-131) in an unstable condition. We took the measured data from Inshas, Cairo, Egypt and compared the concentration of the calculated results with the results obtained from the solution equation at heights of 0.7, 27, and 43 meters. We found that all models are within a factor of two with the observed data from statistical evaluations in unstable conditions, we found that all models fell into a factor of two with the observed data. Whereas with NMSE and FB, the current models correlate better with the observed data.

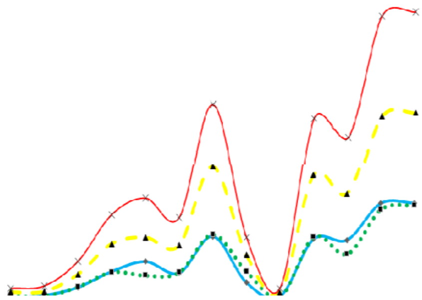

INTRODUCTION

Modelling the atmospheric dispersion of volatile and radioactive gas emissions has a significant contribution to various stages of nuclear technology safety standards, as the majority of industrialized developing countries are increasingly concerned about air pollution. The main causes of air pollution include increased use of automobiles, expansion of industrial facilities, and decreased recycling of industrial waste. Air pollution modelling was relevant to many other fields, from the study of short-term dispersal of species (usually an accidental release in the case of an industrial hazard) to atmospheric chemistry and climate change. Mechanisms, removal mechanisms, topographic features.[1]

The 1954 Monin and Obukhov hypothesis for atmospheric turbulence correctly predicted vertical patterns of turbulence strength. They began by combining the vertical turbulent momentum and heat fluxes into a single quantity with a length dimension, the so-called Monin-Obukhov length.

The air dispersion modeling for the emission of radioactive gases and volatiles made a significant contribution to the nuclear technology safety requirements at various phases, as discussed.[2] The potential harm from a nuclear power reactor (or even a research reactor) was began by solving the advection-diffusion equation, as well as the dispersion and transport of the radioactive cloud in the atmosphere, and eventually the excessive radiation exposure of the general public. Many

* Corresponding author: sawsanibrahim74@yahoo.com

variables determine the area of the radioactive discharge that is affected on the ground or in the atmosphere.[3]

The power of the amount of radiation released, wind speed and direction, temperature, and the physical characteristics of the radioactive substance that was discharged. A 3D model of the atmosphere was presented with energy laws, variable removal rates, and wind speeds. The issue of air pollution dispersion was tackled analytically with varying wind speeds and variable eddy diffusivity for modelling atmospheric dispersion was provided.[4]

It could be assumed that the mean concentration gradient was proportional to the turbulent fluxes of atmospheric air pollution.[5] Several factors influence the area of the ground or the atmosphere that was affected by the radioactive discharge.[6] In the environment of a fundamental rectangle box, the transport equation's mathematical model has a statistical value. [7] Although several limitations were revealed, the Monin-Obukhov theory remains the most trustworthy foundation for all branches of atmospheric modelling by comparison to multiple measurements and advanced computational fluid dynamics data sets.[8]

The three-dimensional rounding equation, a successful digital method, has been developed. These schemas' correctness and effectiveness were described as two test problems. It is possible to use the suggested techniques for physics and geometry nonlinear problems.[9]

In this paper, iodine concentration I^{131} was analyzed at effective heights of 0.7, 27, and 43 meters above the ground with variable vertical eddy diffusivity, but constant wind speed and horizontal and lateral eddy diffusivity, we analytically solved the horizontal diffusion equation in 3D under unstable conditions. Velocity and lateral eddy horizontal propagation are taken as constant.

MATERIAL AND METHODS

The conservation of mass equation, which describes advection, turbulent diffusion, and chemical reactions, provides the basis for the mathematical formulation of the dispersion of air pollution gives the following formulation the time-dependent advection-diffusion equation:[10]

$$\frac{\partial C}{\partial t} + u\frac{\partial C}{\partial x} + v\frac{\partial C}{\partial y} + w\frac{\partial C}{\partial z} = \frac{\partial}{\partial x}\left(k_x\frac{\partial C}{\partial x}\right) + \frac{\partial}{\partial y}\left(k_y\frac{\partial C}{\partial y}\right) + \frac{\partial}{\partial z}\left(k_z\frac{\partial C}{\partial z}\right) + R \tag{1}$$

where: C is pollutant concentration (g/m^3) at points (x, y, z) and u, v, w are components of wind velocity (m/s) and K is the eddy diffusivity whose components are K_x, K_y, and K_z (m^2 /s) along the x, y, and z axes respectively, S and R represent the internal sources or sinks, and removal terms are ignored, so that $S = 0$ and $R = 0$. x, y, and z are horizontal distances from the source. Lateral distance from the source (m) and vertical distance above the source (m) the turbulence contribution appears on the right-hand side. As the average wind field changes from hour to hour, the effect is felt in the advection terms $u\,\partial C/\partial x$ and $v\,\partial C/\partial y$ on the left-hand side, which also contributes to variations in concentration. Thus, turbulent diffusivities are increasing functions of averaging time and z represents turbulent diffusion of material in the y and z directions, respectively. This represents that horizontal advection is much greater than horizontal diffusion, so horizontal diffusion is neglected.

Therefore Eq. (1) is reduced to the time-dependent advection-diffusion equation in three dimensions

$$\frac{\partial C}{\partial t} + u\frac{\partial C}{\partial x} - k_y\frac{\partial^2 C}{\partial y^2} = k_z\frac{\partial^2 C}{\partial z^2} + K_z'\frac{\partial C}{\partial z}. \tag{2}$$

Equation (2) was solved under the following boundary conditions:

$$k_z\frac{\partial C}{\partial z} = 0 \quad \text{at} \quad z = 0, h \tag{2-1}$$

$$u\,C(x, y, z, t) = Q\delta(y)\delta(z - h) \quad \text{at} \quad x = 0 \tag{2-2}$$

$$C\,(x, y, z, t) = 0 \quad \text{at} \quad t = 0, 20\ \text{s} \tag{2-3}$$

$$\frac{\partial C}{\partial y} = 0 \quad \text{at} \quad y = 0, L_y = 0 \tag{2-4}$$

$$\frac{\partial C}{\partial x} = 0 \quad \text{at} \quad x = 0 \quad L_x = 100\ \text{m} \tag{2-5}$$

$$C(x, y, z, t) = \delta(t)\delta(y) \quad \text{at} \quad t, y = 0 \tag{2-6}$$

where δ () is the Dirac delta function, Q is the emission strength of an elevated point source, and h is the effective height of the air pollutant. Condition (2-2) states that the air pollutant is released from the elevated point source of strength Q. Condition (2-3) states that the concentration of the air pollutant is zero for x, y, $z \rightarrow 0$. Condition (2-4) states that the diffusion flux at the lateral coordinate and large distance (L_y) is zero. Condition (2-5) states that the diffusion flux at the horizontal coordinate is zero and L_x is a large constant value of 100 m. Condition (2-6) states that air pollutants are released from the elevated point source. In terms of lateral and horizontal eddy diffusivity (K_x and K_y = 500 m^2/s).[11]

While the vertical eddy diffusivity in unstable conditions in the form is[12]

$$K_z = 0.4\, u_* \, z/0.74 \left(1 - \frac{9\,z}{L}\right)^{-\frac{1}{2}} \quad .$$

Here vertical height (z), Monin-Obukhov length (L), and friction velocity (u_*) [m/s], h is the effective height (0.7 m, 27 m, and 45m).

To solve Eq. (2), it is assumed that: using the variable separation method and assuming the experimental result from Eq. (2) as follows:

$$C(x, y, z, t) = C(x, y, t)\, Z\,(z) \tag{3}$$

where

$$C(x, y, t) = X\,(x)\; Y(y)\; T\,(t)\,, \tag{3-1}$$

where $X\,(x)$ a function of just x, $Y\,(y)$ is a function of just y, and $T\,(t)$ is a function of just t.

To solved the right-hand side of equation (2) by using Eq. (3-1) as follows: deriving equation (3-1) with respect to x, y, and t and substituting it into equation (2) and dividing by X (x), Y (y), and T (t) to equal λ^2, we get the following:

$$\frac{T'(t)}{T(t)} + u\frac{X'(x)}{X(x)} - k_y\frac{Y''(y)}{Y(y)} = -\lambda^2 \tag{3-1-1}$$

where λ^2 is the separation constant of the variables x, y, and t.

Equation (3-1-1) is divided into three equations as follows:

$$T'(t) + \lambda_t^2 T(t) = 0 \tag{3-1-1a}$$

$$X'(x) + \frac{\lambda_x^2}{u} X(x) = 0 \tag{3-1-1b}$$

$$Y''(y) - \frac{\lambda_y^2}{K_y} Y(y) = 0\,. \tag{3-1-1c}$$

To solve Eq. (3-2-1a): integrating Eq. (3-2-1a) with respect to t from 0 to t as follows:

$$T(t) = T(0)e^{-\lambda_t^2 t} \tag{4}$$

where $T(0)$ is the constant of integration.

Substituting from Eq. (2-3) at $t = 0$ in Eq. (4), one gets:

$$T(0) = 1\,. \tag{4a}$$

Substituting from Eq. (2-3) at $t = 20$ s in Eq. (4), one gets

$$\lambda_t^2 = \frac{1}{20}\,. \tag{4b}$$

Substituting from Eqs. (4a) and (4b) in Eq. (4), one gets:

$$T(t) = e^{-\frac{t}{20}} \tag{5}$$

To solve Eq. (3-1-1b): integrating Eq. (3-1-1b) with respect to x from 0 to x, we get:

$$X(x) = X(0)e^{-\frac{\lambda_x^2}{u}x} \tag{6}$$

where $X(0)$ is the constant of integration.

Substituting from Eq. (2-2) at $x = 0$ in Eq. (6), one gets:

$$X(0) = \frac{Q\delta(y)(z-h)}{u} \tag{6a}$$

Substituting from Eq. (2-5) at x= L_x in Eq. (6), one gets:

$$\lambda_x = \sqrt{\frac{u}{x}}\,. \tag{6b}$$

Substituting from Eqns. (6a) and (6b), we get that:

$$X(x) = \frac{Q\delta(y)(z-h)}{u} e^{-1}. \tag{7}$$

To solve equation (3-1-1c): using the Laplace transform on the Eq. (3-1-1c) with respect to y, it becomes as follows:

$$\breve{Y}(y) = \frac{sY(o) - \grave{Y}(o)}{\left(s^2 - \frac{\lambda_y^2}{K_y}\right)} \tag{8}$$

where:

$$\breve{Y}(y) = L_p\{Y(y); y \to s\}, \quad L_p\left(\frac{\partial^2 Y(y)}{\partial y^2}\right) = s^2\breve{Y}(y) - sY(0) - \acute{Y}(0)$$

Substituting from Eq. (2-4)) in Eq.(8), one gets:

$$\grave{Y}(o) = 0. \tag{8a}$$

Substituting from Eq. (8a)) in Eq.(8), one gets:

$$\breve{Y}(y) = \frac{sY(o)}{\left(s^2 - \frac{\lambda_y^2}{K_y}\right)}\,. \tag{8b}$$

Using inverse Laplace transforms on Eq, (8b) becomes:

$$Y(y) = Y(0)\cosh\left(\frac{\lambda_y}{\sqrt{K_y}}\, y\right) = Y(0)\left(\frac{e^{\frac{\lambda_y}{\sqrt{K_y}}y} + e^{\frac{-\lambda_y}{\sqrt{K_y}}y}}{2}\right) \tag{8c}$$

where $\cosh\left(\frac{\lambda_y}{\sqrt{K_y}}\, y\right) = \frac{e^{\frac{\lambda_y}{\sqrt{K_y}}y} + e^{\frac{-\lambda_y}{\sqrt{K_y}}y}}{2}$.

Then:

$$Y(y) = Y(0)\left(\frac{e^{\frac{\lambda_y}{\sqrt{K_y}}y} + e^{\frac{-\lambda_y}{\sqrt{K_y}}y}}{2}\right). \tag{9}$$

Substituting from Eq. (2-4) at $y = L^y$ in Eq. (9), one gets:

$$\lambda_y = \frac{\sqrt{K_y}}{2L_y} \tag{9a}$$

Substituting from Eq. (2-6) at $y = 0$ in Eq. (9), one gets:

$$Y(0) = \delta(t)\delta(y) \quad . \qquad (9b)$$

Substituting from Eqs. (9a) and (9b) in Eq. (9), one gets:

$$Y(y) = \delta(t)\delta(y) \quad \left(\frac{e^{\frac{\lambda_y}{\sqrt{K_y}}y} + e^{\frac{-\lambda_y}{\sqrt{K_y}}y}}{2}\right) \qquad (10)$$

Substituting fromEqns. (5), (7) and (10) in Eq. (3) becomes:

$$C(x, y, t) = \frac{Q\delta(y)(z-h)\delta(t)\delta(y)}{u}\left[\mathrm{Exp}\left(-\left(\frac{\lambda_x^2}{u} + \frac{t}{20} + \frac{\lambda_y y}{2\sqrt{K_y}}\right)\right)\right] \qquad (10\text{-}1)$$

The following are the steps to solve the left side of Eq. (2), where:

$$\because k_z \frac{\partial^2 C}{\partial z^2} = -\frac{\partial K_z}{\partial z}\frac{\partial C}{\partial z}$$

$$K_z = 0.4\, u_* \, z/0.74\left(1 - \frac{9\,z}{L}\right)^{-\frac{1}{2}} \quad , \frac{\partial K_z}{\partial z} = \frac{0.4u_*}{0.74}\left(\frac{(2L - 27z)}{2L\sqrt{1 - \frac{9z}{L}}}\right) \text{ and } \frac{\partial K_z}{K_z\,\partial z} = \frac{(2L - 27z)}{2z(L - 9z)}$$

$$\therefore 0.4\, u_* \, z/0.74\left(1 - \frac{9\,z}{L}\right)^{-\frac{1}{2}}\frac{\partial^2 Z(z)}{\partial z^2} = -\frac{0.4u_*}{0.74}\left(\frac{(2L - 27z)}{2L\sqrt{1 - \frac{9z}{L}}}\right)\left(\frac{\partial Z(z)}{\partial z}\right)$$

$$\frac{\partial^2 Z(z)}{\partial z^2} = \frac{(27z+2L)}{2z(9z+L)}\left(\frac{\partial Z(z)}{\partial z}\right) \qquad (11)$$

Using the substitution approach, because *z* is not present in Eq. (11),:

$$\frac{\partial Z(z)}{\partial z} = P,\ \frac{\partial}{\partial z}\left(\frac{\partial Z(z)}{\partial z}\right) = \frac{\partial P}{\partial z} \qquad (11a)$$

Substitution from Eq. (11a) in Eq. (5) results in:

$$\frac{\partial P}{\partial z} = \left(\frac{(27z+2L)}{2z(9z+L)}\right)P \rightarrow \frac{\partial P}{P} = \left(\frac{(27z+2L)}{2z(9z+L)}\right)\partial z \qquad (11b)$$

$$P = c_1 e^{\int\left(\frac{(27z+2L)}{2z(9z+L)}\right)\partial z} \qquad (11c)$$

When the integral is solved with partial fractions, $\int\left(\frac{(27z+2L)}{2z(9z+L)}\right)\partial z$ become:

$$\int\left(\frac{(27z+2L)}{2z(9z+L)}\right)\partial z = \left(\ln(z) + \ln\sqrt{(L-9z)}\right) - \ln(\sqrt{L}) \qquad (11d)$$

When Eq.(11d) is substituted in Eq.(11c), it results

$$P = c_1\left(z\sqrt{\frac{(L-9z)}{L}}\right) \qquad (11e)$$

Substituting from Eq. (11a) in Eq.(11e) it becomes:

$$\frac{\partial Z(z)}{\partial z} = c_1\left(\frac{z\sqrt{L-9z}}{\sqrt{L}}\right) \qquad (11\ f)$$

Substituting from Eq. (2-1) to Eq. (11 f), we get :

$$c_1 = 1 \qquad (11g)$$

Substituting from Eq. (11g) in Eq. (11f) becomes:

$$\frac{\partial Z(z)}{\partial z} = \left(\frac{z\sqrt{L-9z}}{\sqrt{L}}\right) \qquad (11h)$$

The integrated equation (11h) with respect to *z* becomes:

$$Z(z) = hz - \frac{6\sqrt[3]{L-9z} - 21.6\sqrt[5]{L-9z}}{\sqrt{L}} + c_2 \qquad (12)$$

substitution from Eq. (2-3) in Eq. (12) becomes

$$c_2 = 0 \qquad (12a)$$

Eq. (12) becomes:

$$Z(z) = hz - \frac{6\sqrt[3]{L-9z} - 21.6\sqrt[5]{L-9z}}{\sqrt{L}} \qquad (13)$$

Substituting from Eqs. (10-1) and Eq. (13) in Eq. (3) to get the general Eq. (2) as follows::

$$\frac{C\,(x,y.z,t)}{Q} = \frac{Q\delta(y)(z-h)\delta(t)\delta(y)}{u}\left[\mathrm{Exp}\left(-\left(\frac{\lambda_x^2}{u} + \frac{t}{20} + \frac{\lambda_y y}{2\sqrt{K_y}}\right)\right)\right]\left(hz - \frac{6\sqrt[3]{L-9z} - 21.6\sqrt[5]{L-9z}}{\sqrt{L}}\right); \qquad (14)$$

where the Dirac delta function,[13] is $\delta(z) = \frac{1}{\pi}\sum_{n=1}^{N}\cos n(z) + \frac{1}{2}$ and the $e^{-\lambda' x/u}$ is the radioactive decay for the specified nuclide, λ' is a decay distance of I-131 equals 9.95×10^{-7}.

RESULTS AND DISCUSSION

Calculate the iodine concentration using the analytical solution that is produced (I131). The information used came from research done to gather air samples in erratic environments. At 0.7, 27, and 43 meters above the ground, samples were taken, and emissions were released at those same heights. With respect to (I^{131}), the decay constant is $9.95 \cdot 10^{-7} \cdot s^{-1}$. Emission rates for I-131.he decay constant for (I^{131}). emissions levels for (I-131). Comparison of the anticipated and various procedures for n = 1:13 at t = 20 minutes.[14] The association between the measured concentration and the actual concentration of iodine I_{131} at various downwind distances and effective heights (0.7, 27, and 43 m) is shown in Table 1. Figure 1 shows the comparison between the calculated results and the observed data at heights (0, 7, 27, and 43 meters; the straight line indicates one, while the dashed lines refer to a factor of two. Figure 2. shows the results calculated and observed with the downwind distance at heights of 0.7, 27, and 43 meters. The red line represents the observed concentration, the green line represents a height of 0.7 meters, the blue line represents the concentration at 27 meters, and the yellow line represents the concentration at 43 meters. This comparison of results and distance at various heights is shown. It crosses in two places (134, and 92 meters.

Table 1

Relation between the actual and estimated concentrations at a different downwind distance at effective height (0.7m) and runs

Exp.	Emission Rate	Distance(m)	Concentration (Bq/m3)	
			Observed	Predicated
1	28114286	92	0.025	0.024
2	28700000	96	0.037	0.032
3	1171429	97	0.090	0.085
4	12885714	98	0.200	0.196
5	13471429	99	0.270	0.263
6	140557143	100	0.190	0.186
7	27528571	115	0.450	0.47
8	28524286	132	0.120	0.119
9	28260714	134	0.030	0.027
10	2928571.4	165	0.420	0.424
11	4100000	184	0.420	0.417
12	1171428.6	200	0.670	0.668
13	2342857.1	300	0.670	0.665

Table 2

Relation between the actual and estimated concentrations at a different downwind distance at effective height (27m) and runs.

Exp.	Emission rate	Distance(m)	Concentration(Bq/m3)	
			Observed	Predicated
1	28114286	92	0.025	0.033
2	28700000	96	0.037	0.03
3	1171429	97	0.090	0.094
4	12885714	98	0.200	0.194
5	13471429	99	0.270	0.17
6	140557143	100	0.190	0.191
7	27528571	115	0.450	0.452
8	28524286	132	0.120	0.196
9	28260714	134	0.030	0.027
10	2928571.4	165	0.420	0.437
11	4100000	184	0.420	0.318
12	1171428.6	200	0.670	0.624
13	2342857.1	300	0.670	0.653

Table 3

Relation between the actual and estimated concentrations at a different downwind distance at effective height (43m) and runs

Exp.	Emission rate	Distance(m)	Concentration(Bq/m3)	
			Observed	Predicated
1	28114286	92	0.025	0.033
2	28700000	96	0.037	0.03
3	1171429	97	0.090	0.094
4	12885714	98	0.200	0.194
5	13471429	99	0.270	0.17
6	140557143	100	0.190	0.191
7	27528571	115	0.450	0.452
8	28524286	132	0.120	0.196
9	28260714	134	0.030	0.027
10	2928571.4	165	0.420	0.437
11	4100000	184	0.420	0.318
12	1171428.6	200	0.670	0.624
13	2342857.1	300	0.670	0.653

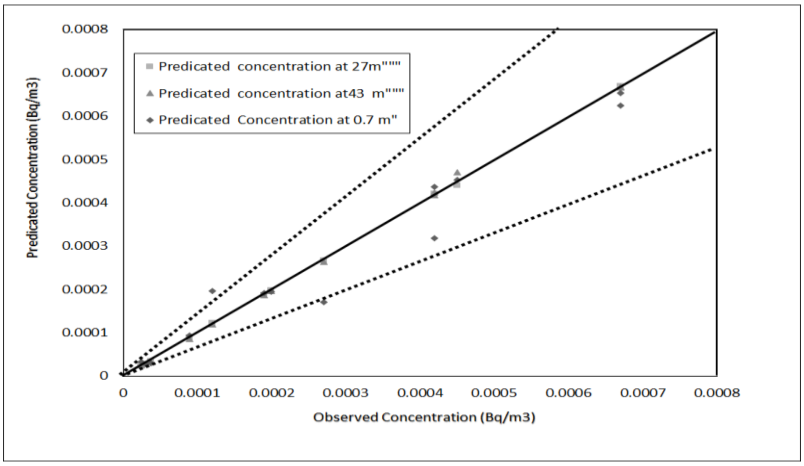

Fig. 1 – shows the comparison between the calculated results and the observed data at heights 0, 7, 27, and 43 meters; the straight line indicates one - one, while the dashed lines refer to a factor of two.

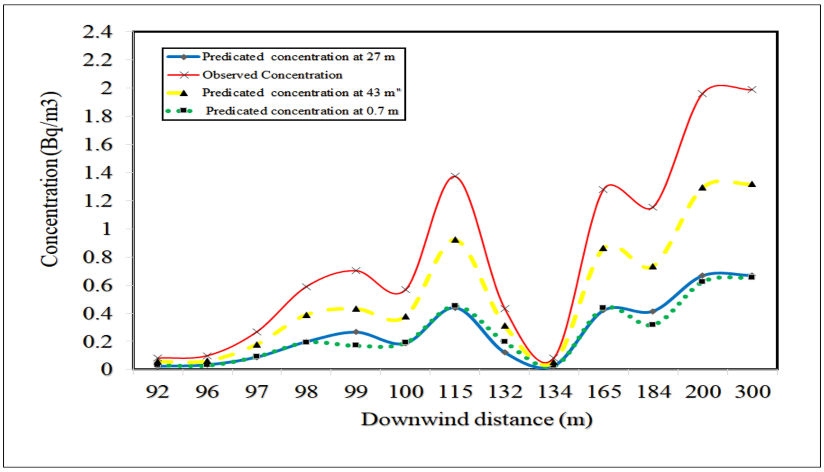

Fig. 2 – The results calculated and observed with the downwind wind distance at heights of 0.7, 27, and 43 meters. The red line represents the observed concentration, the green line represents a height of 0.7 meters, the blue line represents the concentration at 27 meters, and the yellow line represents the concentration at 43 metres.

STATISTICAL ANALYSIS

The statistical method is presented and a comparison will be made between the analytical and statistical results.[15]

Normalized Mean Square Error

$$(\mathrm{NMSE}) = \frac{\overline{(C_p - C_o)^2}}{\overline{(C_p C_o)}}$$

Fraction Bias

$$(\mathrm{FB}) = \frac{(\overline{C_o} - \overline{C_p})}{[0.5(\overline{C_o} + \overline{C_p})]}$$

Correlation Coefficient

$$(\mathrm{COR}) = \frac{1}{N_m}\sum_{i=1}^{N_m}(C_{pi} - \overline{C_p}) \times \frac{(C_{oi} - \overline{C_o})}{(\sigma_p \sigma_o}$$

Factor of Two

$$(\mathrm{FAC2}) = 0.5 \leq \frac{C_p}{C_o} \leq 2.0$$

The standard deviations of Cp and Co are represented by p and o, respectively. Here, the over-bar measurements show the average totals.

The following idealised performance would characterise the ideal model: = FB = 0, and COR = FAC2 = 1.

Table 4

Comparison of different models according to standard statistical performance measurement

Models	NMSR	FB	COR	FAC2
Model at h=0.7m	0.005	0.12	0.99	0.89
Model at h=27m	0.008	0.05	0.96	0.95
Model at h=43m	0.002	0.03	0.93	0.97

Take note of how closely the models we obtained match the observed data by a factor of two. The current models correlate better with the observed data as compared to previous models, according to statistical analyses in NMSE and FB under unstable conditions.

CONCLUSIONS

The equation for diffusion in three dimensions was solved using the separation variable and Laplace transform methods, taking into account that eddy diffusivity along the horizontal and lateral coordinates and wind velocity are respectively constant, while the vertical eddy diffusivity is a function of the vertical height *z*, and the length of Monin-Obukhov *L* has different vertical friction velocity, emission rate and operation of Iodine (I-131) in an unstable condition. We took the measured data from Inshas, Cairo, Egypt and compared the concentration of the calculated results with the results obtained from the solution equation at heights of 0.7, 27, and 43 meters. We found that all results are within a factor of two with the observed data.

From statistical evaluations in unstable conditions, we found that all models fell into a factor of two with the observed data. Whereas with NMSE and FB, the current models correlate better with the observed data.

REFERENCES

1. V. S. Verma, S. Srivastava and M. Agarwal, *South East Asian J. Math. Math. Sc.*, **2011**, *9*, 43–48.
2. D. Moreira, M. Vilhena and J. da Costa Carv, *Ecological Modeling*, **2005**, 189–198.
3. S. Srivastava, M. Agarwal and V. S. Verma, *J. Nat. Acad. Math. Spl.*, **2009**, 189–197.
4. M. Sharan, M. Modani and A. K. Yadav, *Proc. Indian Natn. Sci. Acad.*, **2003**, *69*, 725–744.
5. D. Buske, M. T. Vilhe, T. Tirabassi and B. Bodmann, *J. Environ. Protection*, **2012**, *3*, 1124–1134.
6. D. M. Moreira, T. Toledo, A. Albuquerque, *Rev. Brasileira de Meteorologia*, **2016**, *31*, 202–210.
7. J. Kusuma, A. Ribal and A. G. Mahie, *Int. J. Differential Eq.*, **2018,** Article ID 7597861, 9 pages.
8. T. Foken, *Boundary-Layer Meteorology*, **2006**, *119*, 431–447.
9. M. Saqiba, S. Hasnainb and D. S. Mashatc, *AIP Advances*, **2017**, *7*, 085306.
10. M. Agarwal and A. Tandon, *Appl. Mathem. Modelling*, **2010**, *34*, 2520–2530, https://DOI.Org/10.1016/J.Apm. 2009.11.016
11. C. C. Shirr and L. J. Shieh, *J. Appl. Meteor.*, **1974**, *13*, 185–204.
12. S. R. Hanna, G. A. Briggs and R. P. Hosker Jr, "Handbook on atmospheric diffusion", United States, 1982. Web. doi:10.2172/5591108.
13. IAEA, *Atmospheric Dispersion in Nuclear Power Plant Sitting*, **1980**, S.S. No. 50-SG-S3, IAEA, Vienna.
14. B. Buttkus, "Spectral Analysis and Filter Theory in Applied Geophysics", Springer-Verlag Berlin, Heidelberg GmbH, 2000, Chapter 3.
15. S. R. Hanna, *Atom Environ.*, **1989,** *23*, 1385–1395.